GALAXY INTERNATIONAL INTERDISCIPLINARY RESEARCH JOURNAL (GIIRJ)
ISSN (E): 2347-6915
Vol. 11, Issue 05, May (2023)

LITHIUM CHLORIDE CO-CRYSTAL WITH METHYLENE BLUE: X-RAY DIFFRACTION STUDY AND HIRSHFELD SURFACE ANALYSIS

M. Abdumajidova

V. Kh. Sabirov
Pharmaceutical Institute of Education and Researches, Tashkent, Republic of Uzbekistan.
Correspondence e-mail: munibaxonabdumajidova@gmail.com

ANNOTATION

A co-crystal of lithium chloride with methylene blue chloride was synthesized in order to create a drug with a high therapeutic effect in the treatment of patients with nervous disorders.It is purposed that lithium salts are widely used in neurobiology for many years as a medicine for treatment .A co-crystal of lithium chloride with methylene blue chloride was synthesized in order to create a drug with a high therapeutic effect in the treatment of patients with nervous disorders.

In given paper, synthesis and single crystal X-ray diffraction study of $[Li(H_2O)_4][MB]_2Cl_3{\cdot}4H_2O$ are discussed. Co-crystal was obtained by stirring of the equimilecular amounts od LiCl and MBCl5H2O in distilled water at room temperature. Crystals of the title compound is triclinic: a=7.3090(9), b=17.480(2), c=18.310(2) Å, α= 116.511(14), β= 95.486(11), γ= 96.169(11)°, V=2053.9(5)Å^3, Z =2.Crystal consists of one $[Li(H_2O)_4]^+$ tetrahedral and two planar $[MB]^+$ cations, as well as three chlorine ions and four crystallization molecules of crystallization. The $[MB]^+$ are cations are packed in mutually parallel π···π stacks with sulfur atoms on one side of the stacks. The dominant contribution to total intermolecular interactions of the $[MB]^+$ cationic belongs to intermolecular hydrogen-hydrogen interactions.

Keywords: Iithium chloride, methylene blue, π···π stacking, Alzheimer's disease, X-ray diffraction crystallography.

1. INTRODUCTION

Methylene blue re-emerged on the stage of fame after the experiments of scientists from the I.M. Sechenov 1st Moscow State Medical University, who received positive results in the treatment of patients with COVID-19. Methylene blue Methylene blue consists of a positive aromatic organic molecule - a cation with an electric charge of +1 and a negative anion with an electric charge -1. Commercial methylene blue is produced as methylene blue chloride hydrates ($MB{\cdot}Cl{\cdot}nH_2O$, n=1÷5) compounds (Figure 1).

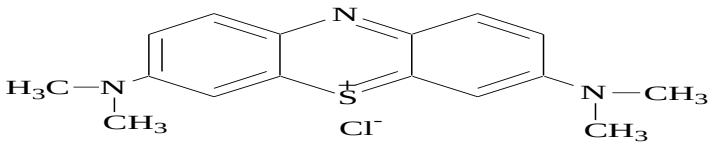

Figure 1. Chemical Formula of Methylene blue

Methylene blue was first produced in 1876 by Heinrich Caro, a German chemist. He worked for the BASF Corporation, to produce a dye for the cotton textile industry. Being an experienced chemist, to create a new waterproof dye, he chose a derivative of phenathiazine, which

simultaneously provided the hydrophobicity and color of the substance, as well as high adhesion of the dye to natural compounds.The substance was first used in medicine by Paul Ehrlich in the mid-1880s, who began using methylene blue in his cell staining experiments, leading to groundbreaking discoveries regarding various cell types.

He has used it for staining bacteria and parasites. One of them is Plasmodiidae, a genus that includes the causative agent of malaria and found that it could be stained with methylene blue. He thought methylene blue could be used to treat malaria. This was a great guess of the great scientist, since if the dye is absorbed by a bacterium, then it may have selectivity for microorganisms and its redox properties could have biological action.He carried out series of the clinical trials which gave positive results, and by the 1890s, methylene blue was being used as an antibacterial drug.

Many reviews and original works are devoted to the properties of methylene blue where detailedinformation about the biological and therapeutic properties of methylene blue are described. Some of them can be mentioned because they form the scientific basis of our research. A review [1] describes the therapeutic effect of MB in the treatment of Alzheimer's disease (AD) and summarizes data suggesting that MB is a promising candidate that can help prevent cognitive decline in AD. The work [2] considers various aspects of the use of MB, and also discusses the problem of rational use of MB in the treatment of COVID-19. The review [3] discusses in detail various forms of methemoglobinemia, biochemical pathways and mechanisms of their occurrence, as well as the use of MB for the treatment of methemoglobinemia.

The review [4] extensively discusses the neuroprotective effects of MB. The work [5] is one of the latest reviews related to MB and its application in medicine.

Our study was motivated by the possibility of using MB in the treatment of AD. The strategy for obtaining benefit compounds is based on the synthesis of MG co-crystals with biologically active compounds.

According to WHO recommendations, co-crystals of two or more drugs can be considered alternative drug substances created using the laws of crystal chemistry in order to obtain new drugs to improve of the physicochemical and biopharmaceutical properties of the active pharmaceutical ingredients (APIs), especially for obtaining new multi-target drugs.

The co-crystals of MBCl with lithium chloride can be considered as a potential drug to use in neuropathology since both compounds have many similar therapeutic properties [6 -10]. Lithium is a type of medicine known as a mood stabilizer. It's used to treat mood disorders such as:

- mania (feeling highly excited, overactive or distracted),
- hypo-mania (similar to mania, but less severe),
- regular periods of depression, where treatment with other medicines has not worked,
- bipolar disorder, where your mood changes between feeling very high (mania) and very low (depression).

In the given paper, the preparation of the co-crystal of lithium chloride with MBCl and its single crystal X-ray diffraction study are discussed. Some intermolecular interactions of $[MB]^+$ cation in co-crystal were studied by CrystalExplorer17 program.

2. Experimental section

2.1. Materials and methods

All reagents were readily available from commercial sources and were used as received without futher purification. Analysis of C, H and O were performed on a German ElementarVario EL instrument.

Yield: 92%. Elemental analysis for $C_{32}H_{52}N_6O_8LiCl_3S_2$(826.20): calcd. C 46.47; H 6.29; N 10.16 %; found: C 46.65; H 6.38; N 10.12%.

2.2. Synthesis and crystallization

Co-crystal of $[Li(H_2O)_4][MB]_2Cl_3{\cdot}8H_2O$ (**I**) was prepared by stirring on magnetic stirrerof equimolar amounts of LiCl (0.01 mol, 0.424 g) and $MB{\cdot}Cl{\cdot}5H_2O$ (0.01 mol, 4.10 g) in distilled water at room temperature for 3 day. The resulting solution was transferred into an evaporating dish and allowed to evaporate slowly at room temperature for one week. The deep blue crystals were purified by recrystallizing in a minimum quantity of ethanol and weighed.

2.3. X-ray diffraction experiments, solution and refinement of the crystal structure

The X-ray data for crystals of **I** was collected on a Rigaku 'XtaLABSynergy HyPix3000' diffractometer at T=293K (CuK_α radiation1,λ = 1.54184 Å, ω scan mode, mirror monochromator) [11].The crystal structure was solved withOLEX2 [12] using the programSHELXT [13], and refined by full-matrix least-squares methods on F^2using the SHELXL refinement package [14]. The resulting crystals has a thin plate shape and form intergrowths. The X-ray experiment was carried out at room temperature. Taken together, these factors did not allow reducing the accuracy of the geometric parameters of molecules to the required accuracy.

All non-hydrogen atoms, with the exception of disordered atomswere refined anisotropically. The H atoms of the C atoms were includedin calculated positions and refined as riding: C–H = 0.95–0.98 Å withUiso(H) = 1.5Ueq(C-methyl) and 1.2Ueq(C) for otherHatoms.

The molecular drawings were plotted with the MERCURY programpackage [15]. Using the software PLATON [16, 17], water molecules ofcrystallization, the hydrogen bonds and short non-bonded contactswere analyzed. Crystal data and data collection and structure refinementdetails for **I** are summarized in the Table 1. Readers can receive the coordinates atoms and other information from author.

Table 1.Crystal data and structure refinement for (I)

Identification code	exp_2558_LiSETRAT	μ/mm^{-1}	3.413
Empirical formula	$C_{32}H_{52}N_6O_8LiCl_3S_2$	F(000)	872.0
Formula weight	826.20	Crystal size/mm^3	0.3 × 0.2 × 0.1
Temperature/K	293(2)	Radiation	CuKα (λ = 1.54184)
Crystal system	triclinic	2Θ range for data collection/°	5.466 to 143.12
Space group	P-1	Index ranges	-8 ≤ h ≤ 8, -21 ≤ k ≤ 18, -21 ≤ l ≤ 22
a/Å	7.3090(9)	Reflectionscollected	20475
b/Å	17.480(2)	Independent reflections	7880 [R_{int} = 0.3339, R_{sigma} = 0.4842]
c/Å	18.310(2)	Data/restraints/parameters	7880/0/493
α/°	116.511(14)	Goodness-of-fit on F^2	0.918
β/°	95.486(11)	Final R indexes [I>=2σ (I)]	R_1 = 0.1291, wR_2 = 0.2232
γ/°	96.169(11)	Final R indexes [all data]	R_1 = 0.4341, wR_2 = 0.3860
Volume/Å^3	2053.9(5)	Largest diff. peak/hole / e Å^{-3}	0.34/-0.37
Z	2	μ/mm^{-1}	1.336

ρ_{calc}g/cm^3	1.336	Crystal size/mm^3	0.3 ×0.2 × 0.1

2.4. Hirshfeld surfaces calculations

Hirshfeld surfaces and related two-dimensional fingerprint plots were generated for the title compound based on the crystallographic information file (CIF) using CRYSTALEXPLORER [18, 19]. The 2D fingerprint plots generated by using the standard 0.6–2.6 Åview with the de and di distance scales are displayed on the graphaxes [20]. The surface transparency enables the display of thestructure of the cation.

3. Results and discussions

3.1. Description of molecular and crystal structures

Crystal structure **I**is built from one $[Li(H_2O)_4]^+$ tetrahedraland two planar $[MB]^+$ cations, as well as three Cl^- anions and four water of crystallization (Fig. 1). The $[Li(H_2O)_4]^+$ tetrahedron is surrounded by three water molecules and two Cl^- ions forming with them hydrogen bonds. The Li-O_w bond lengths are in the range of 1.88(3) - 2.04 Å and the O_w-Li-O_w bond angles are in the range of 99.4(17) - 121.8(19)° (Table 2).

In the crystal structure of I, the adjacent planar [MB]+ cations are located almost in parallel planes. The dihedral angle between two planes is 2.7°. Contrary to other MB compounds with antiparallel orientation of cations, in this crystal the $[MB]^+$ cations are packed in parallel planes with the sulfur atom on one side. In this case, the MB cations are more shifted relative to each other (Fig. 2, 3). The centroid-centroid distance between the thiazine rings of neighboring $[MB]^+$ cations is 4.67 Å, and the average interplanar distance is 3.58 Å.

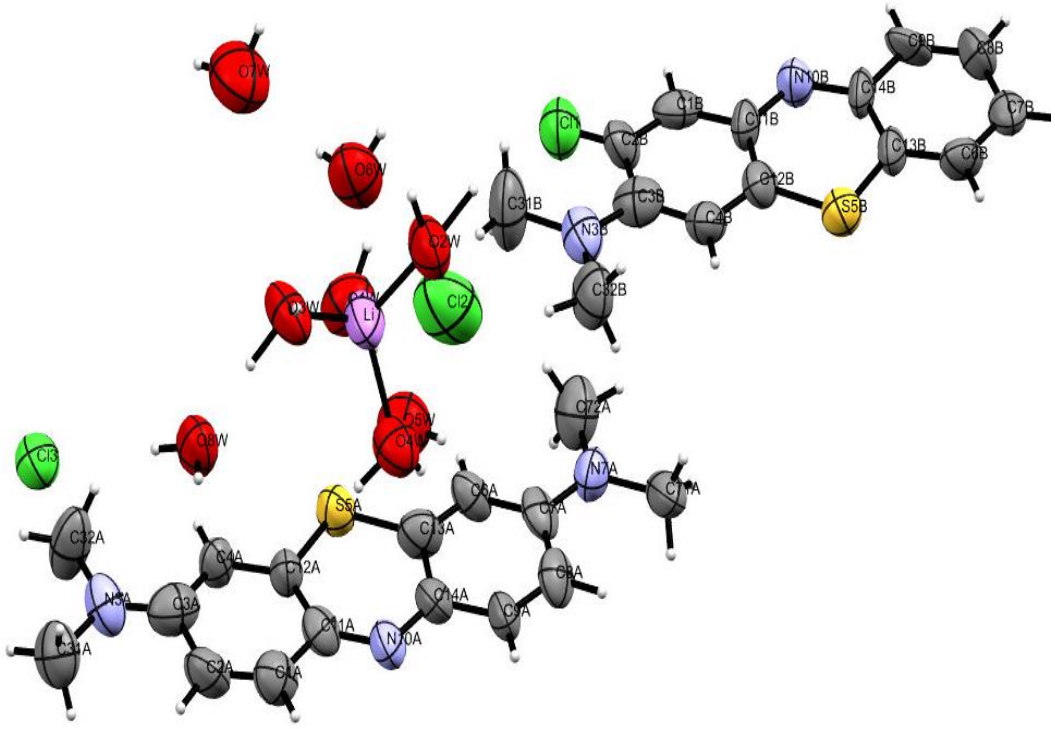

Figure 1. Molecular structure and atom numbering scheme for the asymmetric unit of **I**. Displacement ellipsoids are drawn at the 50% probability level.

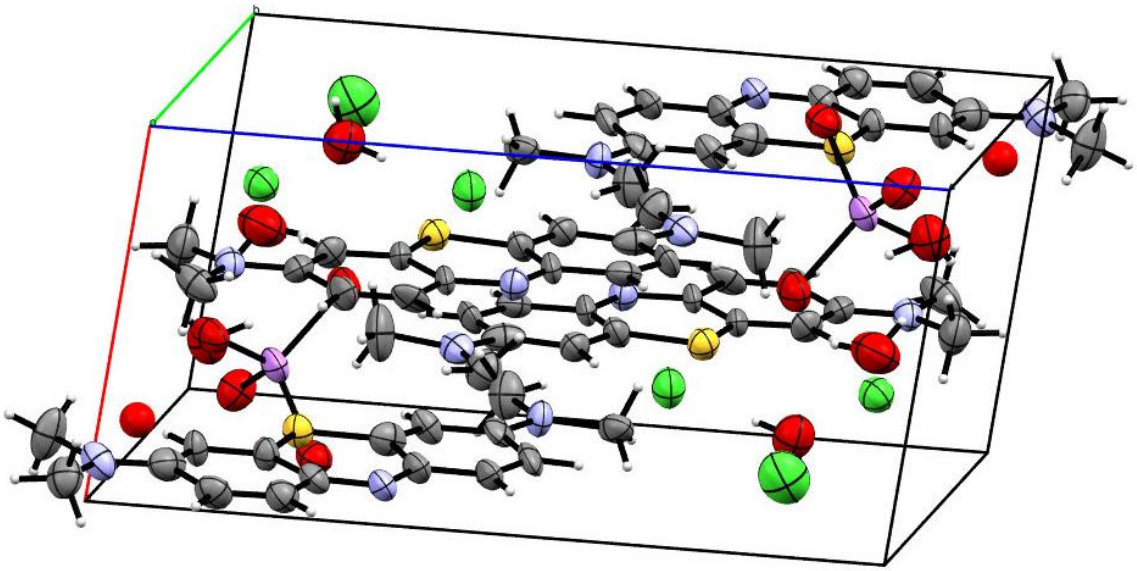

Figure 2. Crystal packing of the title compound. Short contacts and hydrogen bonds are not shown for clarity.

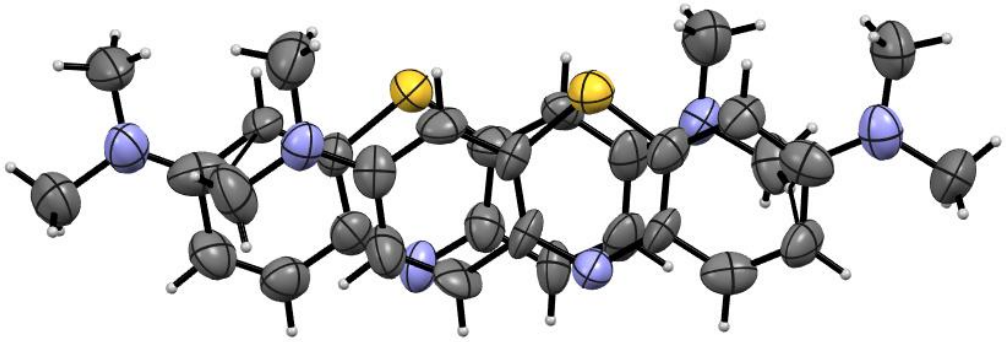

Figure 3. Mutual parallel orientation two neighboring [MB]+ cations.

Large uncertainties in the determination of the bonds lengths and angles do not allow us to judge the increase or decrease in these parameters. Selected bond lengths and angles are shown in Table 2. These parameters are indicators of the realization of one or another resonantforms of the $[MB]^+$ cation.

Table 2.Selected bond lengths and angles forI.

Atom	Atom	*d*, Å	Atom	Atom	*d*, Å
Li	O_w	1.88(3); 1.91(4); 2.04(4);1.96(3)			
S5A	C13A	1.726(17)	S5B	C13B	1.761(15)
S5A	C12A	1.748(15)	S5B	C12B	1.703(16)
N3A	C3A	1.32(2)	N3B	C3B	1.40(2)
N10A	C14A	1.339(18)	N10B	C14B	1.314(17)
N10A	C11A	1.315(18)	N10B	C11B	1.374(18)
N7A	C7A	1.362(19)	N7B	C7B	1.345(19)

Angle			ω, °	Angle			ω,°
O_w	Li	O_w			99.4(17) - 121.8(19)		
C12A	S5A	C13A	104.9(8)	C11A	N10A	C14A	121.3(15)
C12B	S5B	C13B	102.4(8)	C11B	N10B	C14B	122.8(13)

The structural units of crystal **I** are linked into 3D - network by a system of hydrogen bonds and weak intermolecular interactions, the geometric parameters of which are given in Table 3.Water molecules, as shown in Table 3, are the main participants of the 3D - network in the crystal packing. The $[MB]^+$ cationsparticipate in four hydration bonds: two with chlorine ions and two with water molecules.The N(10) and S(5) atoms of the thiazine ring form intermolecular contacts where H…N and H…S separations are longer than the sum of the van der Waals radiicorresponding atoms.

Table 3. Hydrogen-bonding geometry (Å, °).

D --- H....A	D - H	H...A	D...A	D-H...A	Symmetry
O3w–H...O8*w*	1.1	1.70	2.77(2)	170	
O3w–H...Cl3	1.0	2.50	3.17(2)	121	[1-*x*, -*y*, -*z*]
O1w –H...O5*w*	1.05	1.72	2.77(2)	173	
O1w–H. ..O6*w*	1.04	2.14	2.98(3)	137	
O8w–H...Cl3	0.85	2.33	3.17(1)	171	
O4w–H...Cl1	0.98	2.25	3.17(1)	157	[1+*x*, *y*, *z*]
O4w–H...Cl3	0.95	2.31	3.26(1)	175	[2-*x*, *y*, *z*]
O6w –H…O7*w*	0.85	2.34	3.07(3)	145	[1-*x*, 1-*y*, -*z*]
O6w–H...O7*w*	0.85	2.07	2.90(3)	168	
O2w–H...Cl3	1.13	2.31	3.27(2)	141	[1-*x*, -*y*, -*z*]
O7w –H...O6*w*	0.85	2.27	3.07(3)	156	[1-*x*, 1-*y*, -*z*]
O7w –H...Cl2	0.85	2.74	3.07(2)	105	[2-*x*, 1-*y*, -*z*]
O5w–H...Cl2	0.85	2.67	3.08(2)	111	
O5w–H...Cl1	0.85	2.44	3.19(2)	147	[*x*, 1+*y*, *z*]
C6B–H...Cl3	0.93	2.67	3.57(2)	163	[*x*, 1+*y*, 1+*z*]
C2A–H...Cl2	0.93	2.73	3.60(2)	157	[*x*, -1+*y*, *z*]
C4A–H...O8*w*	0.93	2.48	3.35(2)	154	
C31A–H...O5*w*	0.96	2.56	3.50(2)	166	[2-*x*, -*y*, -*z*]

3.2. Analysis of the Hirshfeld surfaces

The CRYSTALEXPLORER17 software is a powerful instrument for Hirshfeld surface analysis, visualization and quantative analysis of molecular crystals. It allows to study hydrogen bonds and weak intermolecular interactions in the crystal.

The Hirshfeld surfaces areused to quantify and visualize the close intermolecularcontacts responsible for the hydrogen bonds and the specificnon-bonded interactions in a crystal structure. Intermolecularcontacts closer than the sum of their van der Waals radii are highlighted in red on the d_{norm} surface,while contacts with a larger distance are highlighted inblue and contacts with distances near the sum of van derWaals radii are white (Figure 4).

As in others compounds of MB, on the d_{norm}(Fig. 4b) surfaces of the $[MB]^+$cations of **I**, white andblue spots predominate. On the shape index (Fig. 4c), convex blueregions represent hydrogen donor groups and concave redregions represent hydrogen acceptor groups. The intermolecularπ…π stacking interactions between the adjacent$[MB]^+$ cations are also evident on the shape index surface (Fig.4d) as red and blue triangles.

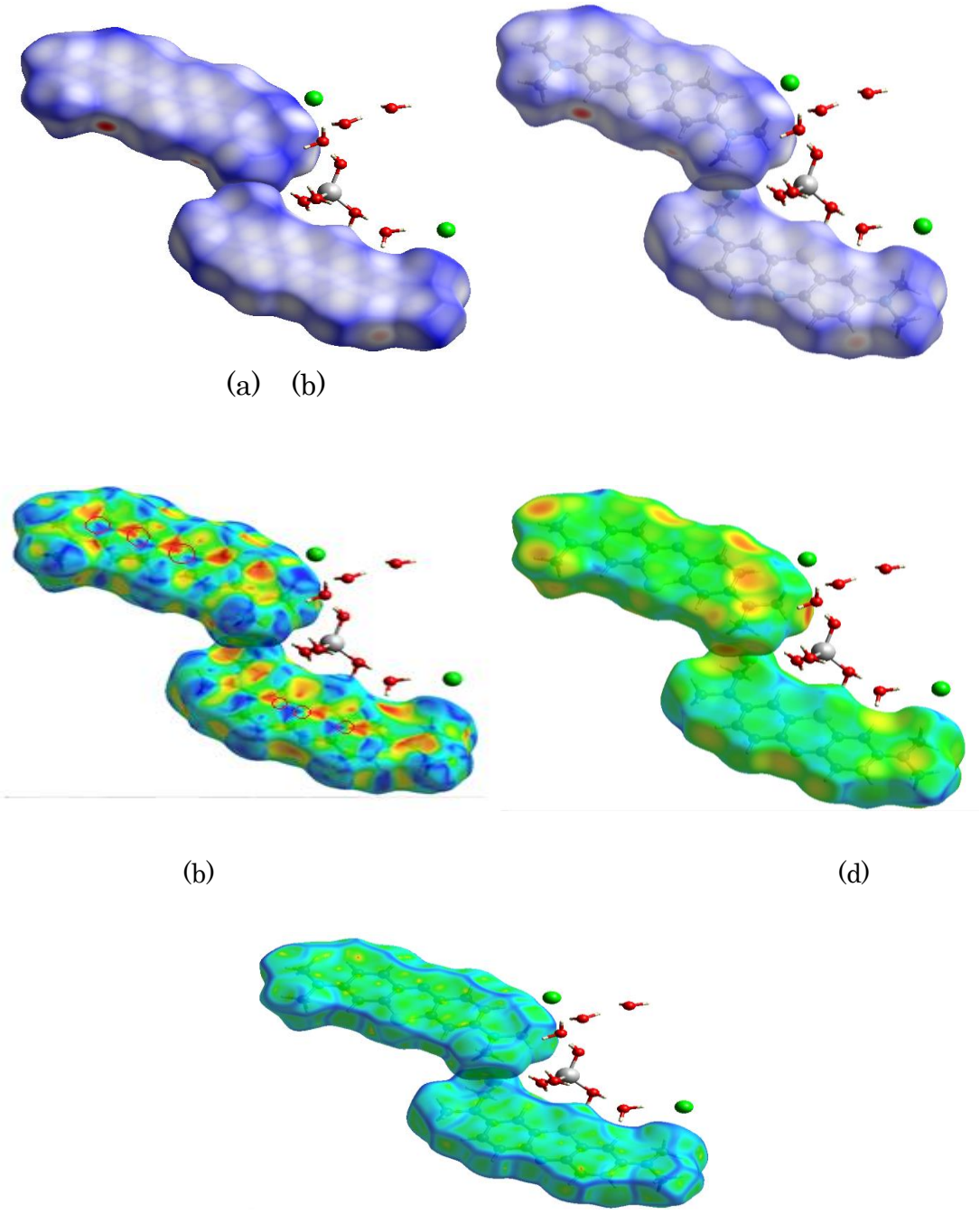

(a) (b)

(b) (d)

(e)

Figure 4. Hirshfeld surfaces of the $[MB]^+$ cations in the structure of **I**mapped with (a) none, (b) d_{norm}, (c) shape index, (d) d_e and (e) curvedness.

The 2D-fingerprint of the Hirshfeld surface represents a power method in the framework of the CRYSTALEXPLORER17 for summarizing the complex information contained in a molecular crystal structure into a single, unique full colour plot, which provides a 'fingerprint' of the

intermolecular interactions in the crystal. Derived from the Hirshfeld surface, these 2D-fingerprint plots provide a visual summary of the frequency of each combination of d_e and d_i across the surface of a molecule, so they not only indicate which intermolecular interactions are present, but also the relative area of the surface corresponding to each kind of interaction.

The overall 2D–fingerprint plot for the compound **I**and those delineated into H···H, H···C, C···C, N···H and S···H contacts are illustrated in Fig. 5 and 6; the percentage contributions from the different interatomic contacts to the Hirshfeld surfaces are as follows (A/B): H···H 49.7/54,9 %, H···C 11.1/10.5 %, C···C 9.1/9.7 %, N···H 5.2/5.5 % and H···S/S···H 5.5/4.9 %. The percentage contributions for the other intermolecular contacts are less than 5% in the Hirshfeld surface mapping. 2D fingerprint plots show that the and H···H and H···C/C…H contacts make the main contribution to the interatomic interactions. This result corresponds to the atomic structure of the MB cation.

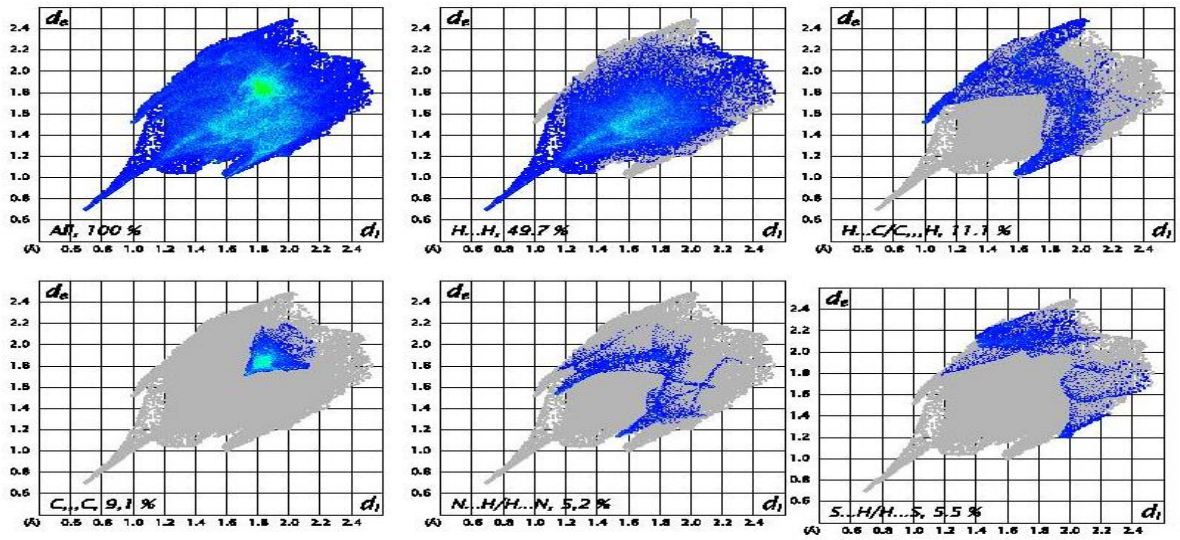

Figure 5. 2D - fingerprint plots for $[MB(A)]^+$ cation in crystal **I**.

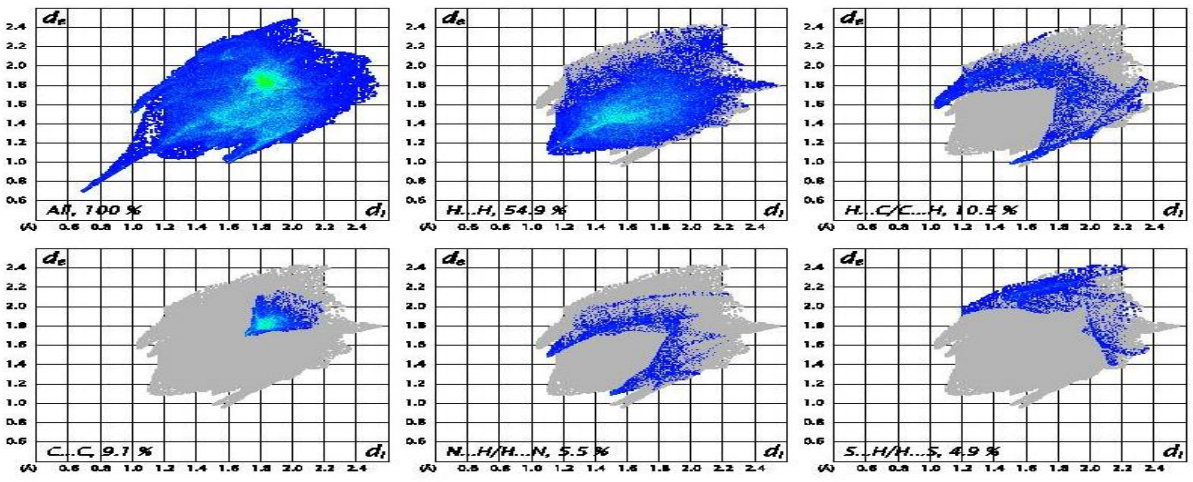

Figure 6. 2D - fingerprint plots for $[MB(B)]^+$ cation in crystal **I**.

3.3. Intermolecular interaction energy calculations

MB dimerization and polymerization in the various solutions has been investigated intensively for many years [22 - 25].

In crystalline MB compounds, MB stacking occurs due to π...π stacking of $[MB]^+$ cations in the crystal packing. However, as noted in work [26], the energy aspects of this phenomenon are still missing.

In this work, intermolecular interaction energy between parallel oriented MB]$^+$ cations has been calculated using of the CE-3LYP/6-31G(d,p) levels of theory. According calculations the interaction energy between two adjacent $[MB]^+$ cations is -57.1 kJ/mol (Table 5). resented values of the total energy components show that the E_{dis} dispersion energy is greater than the repulsion energy and plays a significant role in the formation of the π···π stacking in the crystal structure.

Table 5. Interaction energy between two parallel neighboring $[MB]^+$ cations in the srystal structure of **I**.

	N	Symop	R	Electron Density	E_ele	E_pol	E_dis	E_rep	E_tot
	1	-	4.64	B3LYP/6-31G(d,p)	-1.45	-19.55	-81.2	45.1	-57.1

4. CONCLUSIONS

The single crystal X-ray diffraction analysis of salt $[Li(H_2O)_4][MB]_2Cl_3{\cdot}4H_2O$ showed that the compound has an ionic structure and consists of tetrahedral $[Li(H_2O)_4]^+$cation and two planar $[MB]^+$ cations, as well as three chlorine ions and four crystallization molecules of crystallization.A and B, as well as water molecules. The $[MB]^+$ are cations are packed in mutually parallel π···π stacks with sulfur atoms on one side of the stacks. The dominant contribution to total intermolecular interactions of the $[MB]^+$ cationic belongs to intermolecular hydrogen-hydrogen interactions. The Hirshfeld surfaces analysis showed that the H···H and H···C interactions make dominant contribution into total intermolecular interactions. According to intermolecular interaction energy, calculated in the framework CRYSTALEXPOLRER17 program, the total energy of the intermolecular interaction equal to E_{tot} is -57.1 kJ/mol. The dispersion energy E_{dis} is greater than the other energies and plays a major role in the π···πstacking of the $[MB]^+$ cations.

REFERENCES

1. Murat Oz, Dietrich E. Lorke, George A. Petroianu.. Methylene blue and Alzheimer's disease. Biochemical Pharmacology 78 (2009) 927–932.

2. Saikrupa B. V. ,Muthukumar Mani, Kavya S. , Suma P Kumar. Rational Use of Methylene Blue in COVID-19 Treatment.

3. R.Manivannan, S.Kameshwaran, V.Srividhya, R. Praveen raj, R. Pravin. A comprehensive review on methemoglobinemia. *Int. J. of Allied Med. Sci. and Clin. Research.* 2021. 9(2), 108-112.

4. Ethan Poteet, Ali Winters, Liang-Jun Yan, Kyle Shufelt, Kayla N. Green, James W. Simpkins1, Yi Wen, Shao-Hua Yang. Neuroprotective Actions of Methylene Blue and Its Derivatives. *PLoS ONE. 2012. 7(10), 48279*. doi:10.1371/journal.pone.0048279

5. YarenKayabaşı, OytunErbaş. Methylene blue and its importance in medicine. *D. J. Med. Sci.* 2020. 6(3). 136-145. doi: 10.5606/fng.btd.2020.25035

6. Robert Haussmann,Felix Noppes,Moritz D Brandt,Michael Bauer,Markus Donix. Lithium: A therapeutic option in Alzheimer's disease and its prodromal stages? Neurosci.Lett. 2021. 24;760:136044.doi: 10.1016/j.neulet.2021.136044.
7. RobertHaussmann,FelixNoppes,MoritzD.Brandt,MichaelBauer,MarkusDonix. Minireview: Lithium: a therapeutic option in Alzheimer's disease and its prodromal stages? NeuroscienceLetters. 2021. 760,24 August 2021, 136044.
8. J. K. Rybakowski. Lithium and Alzheimer's Disease: Experimental, Epidemiological, and Clinical Findings. In book Alzhheimar's Disease. Ed. J. Dorszewska& W. Kozubski. 2017. DOI: 10.5772/intechopen.74239.
9. Janusz K.Rybakowski. Lithium. Eur.Neuropsychopharm.2022. 57,86-87.
10. S.H. Naughton, W. D. Beck, Z. Wei, G. Wu, A. V. Terry. Multifunctional compounds lithium chloride and methylene blue attenuate the negative effects of diisopropylfluorophosphate on axonal transport in rat cortical neurons. Toxicology. 2020. 431, 152379.
11. CRYSALIS PRO Software System (version 1.171.40.84a). Intelligent Data Collection and Processing Software for Small Molecule and Protein Crystallography; Rigaku Oxford Diffraction: Yarnton, Oxfordshire (UK), 2020.
12. Dolomanov O. V., Bourhis L. J., Gildea R. J., Howard J. A. K., Puschmann H. J. Appl. Crystallogr. 2009, 42, 339–341.
13. Sheldrick G. M. Acta Crystallogr. 2015, A71, 3–8.
14. Sheldrick G. M. Acta Crystallogr. 2015, C71, 3–8.
15. Macrae C. F., Bruno I. J., Chisholm J. A., Edington P. R., McCabe P., Pidcock E., Rodriguez-Monge L., Taylor R., van de Streek J., Wood P. A. J. Appl. Crystallogr. 2008, 41, 466–470.
16. Spek A. L. Acta Crystallogr. 2015, C71, 9–18.
17. Spek A. L. Acta Crystallogr. 2009, D65, 148–155.
18. Spackman M. A., Jayatilaka D. CrystEngComm 2009, 11, 19–32.
19. Spackman P. R., Turner M. J., McKinnon J. J., Wolff S. K.,
20. Grimwood D. J., Jayatilaka D., Spackman M. A. J. Appl. Crystallogr. 2021, 54, 1006–1011.
21. Spackman M. A., McKinnon J. J. CrystEngComm 2002, 4, 378–392.
22. Rabinowich E.; Epstein L. *Polymerization of Dyestuffs in Solution. Thionine and Methylene Blue. J.A.C.S.* 1941. *63, 69–78.*doi: 10.1021/ja01846a011
23. Lewis G. N.; Goldschmid O.; Magel T. T.; BigeleisenJ. Dimeric and other forms of methylene Blue: absorption and fluorescence of the Pure Monomer. *J. Am. Chem. Soc.* 1943. 65, 1150–1154. doi:10.1021/ja01246a037
24. Bergmann K., O'Konski T. Spectroscopic study of methylene blue with montmorillonite. A spectroscopic study of methylene blue monomer, dimer, and complexes with montmorillonite. *J. Phys. Chem.* 1963. 67, 2169–2177. doi: 10.1021/j100804a048
25. Florence Ng.; Naorem H. Dimerization of methylene blue in aqueous and mixed aqueous organic solvent: A spectroscopic study. *J. Mol. Liq.* 2014. 198, 255–258. doi: 10.1016/j.molliq.2014.06.030
26. Batsanov A. S. Weak interactions in crystals: old concepts, new developments. Acta Cryst. 2018). E74, 570–574.